Comparative Genomics of Six *Juglans* Species Reveals Patterns of Disease-associated Gene Family Contractions.

Alex Trouern-Trend[1*], Taylor Falk[1*], Sumaira Zaman[1], Madison Caballero[1], David B. Neale[2], Charles H. Langley[4], Abhaya Dandekar[2], Kristian A. Stevens[3,4+], Jill L. Wegrzyn[1+]

[1]Department of Ecology and Evolutionary Biology, University of Connecticut, Storrs, CT, USA
[2]Department of Plant Sciences, University of California Davis, Davis, CA, USA
[3]Department of Computer Science, University of California Davis, Davis, CA, USA
[4]Department of Evolution and Ecology, University of California Davis, Davis, CA, USA

[*]Joint First Authors
[+]Joint Corresponding Authors

Journal: The Plant Journal (Resource)

ABSTRACT

Juglans (walnuts), the most speciose genus in the walnut family (Juglandaceae) represents most of the family's commercially valuable fruit and wood-producing trees and includes several species used as rootstock in agriculture for their resistance to various abiotic and biotic stressors. We present the full structural and functional genome annotations of six *Juglans* species and one outgroup within Juglandaceae (*Juglans regia*, *J. cathayensis*, *J. hindsii*, *J. microcarpa*, *J. nigra*, *J. sigillata* and *Pterocarya stenoptera*) produced using BRAKER2 semi-unsupervised gene prediction pipeline and additional in-house developed tools. For each annotation, gene predictors were trained using 19 tissue-specific *J. regia* transcriptomes aligned to the genomes. Additional functional evidence and filters were applied to multiexonic and monoexonic putative genes to yield between 27,000 and 44,000 high-confidence gene models per species. Comparison of gene models to the BUSCO embryophyta dataset suggested that, on average, genome annotation completeness was 89.6%. We utilized these high quality annotations to assess gene family evolution within *Juglans* and among *Juglans* and selected Eurosid species, which revealed significant contractions in several gene families in *J. hindsii* including disease resistance-related Wall-associated Kinase (WAK) and *Catharanthus roseus* Receptor-like Kinase (CrRLK1L) and others involved in abiotic stress response. Finally, we confirmed an ancient whole genome duplication that took place in a common ancestor of Juglandaceae using site substitution comparative analysis.

KEYWORDS:

walnut, wingnut, *Juglans*, Juglandaceae, genome annotation, comparative genomics, whole genome duplication, phenology, disease resistance, crop genomics

SIGNIFICANCE

High-quality full genome annotations for six species of walnut (*Juglans*) and a wingnut (*Pterocarya*) outgroup were constructed using semi-unsupervised gene prediction followed by gene model filtering and functional characterization. These annotations represent the most comprehensive set for any hardwood genus to date. Comparative analyses based on the gene models uncovered rapid evolution in multiple gene families related to disease-response and a whole genome duplication in a *Juglandaceae* common ancestor.

INTRODUCTION

It is anticipated that new genomic resources for *Juglans* (walnuts) will lead to improved timber and nut production by accelerating development of advanced agriculture, breeding efforts, and resource management techniques for the genus (Resende *et al*. 2012). Already, these practices are beneficiaries of the genomic analyses and tool development potentiated by the growing pool of *Juglans* sequence data (Martínez-García *et al.* 2017; Bernard *et al.* 2018; Marrano *et al.* 2018,

Famula *et al.* 2019). The recent publication of the unannotated draft reference genomes of six *Juglans* species: *J. nigra* (Eastern black walnut), *J. hindsii* (Hinds' black walnut), *J. microcarpa* (Texas walnut), *J. sigillata* (iron walnut), *J. cathayensis* (Chinese walnut), *J. regia* (Persian or English walnut) and a member of the sister group to *Juglans*, *Pterocarya stenoptera* (Chinese wingnut) (Stevens *et al*. 2018) greatly expands the existing resource and provides an unprecedented opportunity to apply tools such as genomic selection to the Juglandaceae. The genomes considered are Eurasian and North American species from across the three sections of the genus, *Cardiocaryon*, *Dioscaryon* (syn. sect. *Juglans*) and *Rhysocaryon* (Figure 1). These species were selected for their historical and agricultural importance and for their phylogenetic placements, which span the breadth of the genus. The North American species *J. nigra*, *J. hindsii*, and *J. microcarpa* are members of sect. *Rhysocaryon* and grow in riparian forests in the eastern, western and southern United States, respectively. *J. hindsii* and *J. microcarpa* are distributed in moderately dispersed populations. Conversely, *J. nigra*'s range is more contiguous and expansive and overlaps with northeastern distribution of *J. microcarpa*. Among these, *J. nigra* is especially valued for its high quality timber, cold-hardiness, and disease resistance (Beineke 1983; Settle *et al*. 2015; Chakraborty *et al*. 2015; Chakraborty *et al.* 2016). *J. hindsii* is associated with vigor, drought tolerance, and resistance to *Armillaria* root rot (honey fungus) (Buzo *et al.* 2009). The need for disease-resistant and climate-tolerant cultivars for nut production has driven the use of *J. nigra, J. hindsii* and *J. microcarpa* in hybridization trials (Browne *et al.* 2015). These species contribute resistance to many soilborne pathogens, including *Phytophthora* and a range of nematodes.

The sampled Eurasian species include *J. regia*, the predominant nut producer of all cultivated *Juglans*. *J. regia*'s western range continues into Southeastern Europe, an impressive relic of silk road trading that underlines its agricultural suitability (Pollegioni *et al.* 2015). *J. sigillata* is phylogenetically adjacent to *J. regia* as the only other species of sect. *Dioscaryon*, and, like *J. regia*, is valued for both its timber and nut (Weckerle *et al.* 2005). Despite their divergent morphology, which includes number of leaflets and nut characteristics, a growing body of molecular evidence suggests that *J. regia* and *J. sigillata* may not qualify as separate species (Gunn *et al*. 2010; Zhao *et al*. 2018). *J. sigillata* grows sympatrically with *J. regia* and *J. cathayensis* (sect. *Cardiocaryon*) in southwestern China, but the distribution of *J. cathayensis* extends beyond the sympatric zone several hundred kilometers eastward to the coastline and northward towards the the Gobi desert. *J. cathayensis* is endangered in its natural range in China (Zhang *et al.* 2015) and is evaluated in breeding programs for its resistance to lesion nematodes. The outgroup, *P. stenoptera* is also native to southeastern China and is used for ornamental planting, timber, and medicinal extracts. *P. stenoptera* has been integrated into hybridization trials as a non-viable rootstock for its resistance to *Phytophthora* (Browne *et al*. 2011).

Stevens *et. al* (2018) annotated a set of microsyntenic regions containing polyphenol oxidase loci to confirm a gene duplication in an ancestral *Juglans*. Here, we describe the full gene annotations of these diploid genomes, a critical missing component to their full utilization as a genomic resource. We demonstrate their utility by investigating two intriguing evolutionary questions. First, we look at the origins and evolutionary relationship of genes families expanded in *Juglans*. Second, we leverage the annotations for a comparative genomic analysis to date an ancient whole genome duplication in an ancestral species of Juglandaceae.

METHODS

Repeat Library Generation and Softmasking

The seven assemblies, ranging in size from 600 Mb to just under 1 Gb (2n=32) were assessed for repeat content (Stevens *et al*. 2018). Scaffolds and contigs less than 3Kbp in length were removed from the assemblies prior to annotation. RepeatModeler (v1.0.8) was used to construct a repeat library through a combination of *de novo* and structural prediction tools wrapped into the pipeline (Smit and Hubley, 2008). RepeatModeler provided base annotations for the repeat elements (Table S1) and generated a consensus library that was used as input to Repeatmasker (v4.0.6) to generate softmasked genomes (Smit *et al*. 2013).

Structural Annotation

After softmasking, a set of 19 independent *J. regia* tissue-specific libraries described in Chakraborty *et al* (2015) were aligned to the reference genomes via TopHat2 (v2.1.1) (Kim *et al*. 2013). The Illumina 85bp PE sequences were independently quality controlled for a minimum length of 45bp and a minimum Phred-scaled quality score of 35 via Sickle (v. 1.33) prior to alignment. Independent alignment files were sorted and provided to Braker2 (v2.0) which generated a hints file for semi-supervised training of the *ab initio* gene prediction package, Augustus (Stanke *et al*. 2008). Braker2 utilizes RNA-Seq reads directly to inform gene prediction and deduce the final models (Hoff *et a*l. 2016). The annotation files (GFF) produced were processed by gFACs, to filter out incomplete or improbable gene models on the bases of completion (identifiable start and stop codons) and canonical gene structure (micro-exons and micro-introns < 20bp are filtered to reduce erroneous models). The gFACs package also resolves conflicting models and reports splice site statistics as well as other basic gene structure statistics (Caballero and Wegrzyn, 2018).

Functional Annotation

The EnTAP functional annotation package was employed to remove unlikely gene models and provide provisional functional information (Hart *et al*. 2018). Multi-exonic and mono-exonic gene models were subjected to different functional filtering pipelines that each utilized EnTAP. For multi-exonic genes, EnTAP (v 0.8.1) was provided three curated databases (NCBI's Plant

115 Protein (release 87), NCBI's RefSeq Protein (release 87), and UniProtKB/Swiss-Prot) for
116 similarity search (50% target and query coverage; Diamond E-value .00001), followed by gene
117 family assignment via the EggNOG database and EggNOG-mapper toolbox (Jensen *et al.* 2008).
118 Associations to gene families provided the basis for Gene Ontology term assignment,
119 identification of protein domains (PFAM), and associated pathways (KEGG) (Finn *et al.* 2014;
120 Ashburner *et al.* 2017). Multi-exonics were removed from the set if they had neither sequence
121 similarity search result nor gene family assignment. Mono-exonic genes are typically over-
122 estimated in the process of *ab initio* genome annotation. To reduce this effect, they were aligned
123 to a custom curated database of monoexonic genes from other plant species using 80% query
124 coverage and 80% target coverage cutoffs in an independent similarity search through EnTAP.
125 EggNOG and PFAM were used in mono-exonic gene model filtering as they were for multi-
126 exonic filtering. After the first round of filters, InterProScan (v5.25) was used to confirm gene
127 family assignment and protein domains in monoexonic gene models. Gene models without
128 InterProScan annotations were removed from the monoexonic set. For each species, the filtered
129 multi-exonic and mono-exonic gene sets were combined and passed back to gFACs to generate
130 a statistical profile and consistent annotation file in gene transfer format (GTF). Finally, gene
131 models that annotated with domains specific to retroelements were further filtered from the
132 final annotations based upon Pfam database descriptions. The entire set of filtered gene models
133 was evaluated for completeness. BUSCO (v3.0.2) was used with default parameters and the
134 embryophyta reference set of 1440 orthologs for this purpose (Simão *et al.* 2015).
135
136 *Gene Family Classification and Evolution*
137 The proteins derived from the filtered genome annotations of each species were processed with
138 OrthoFinder-Diamond (v1.1.10) to provide information about orthologous gene families.
139 OrthoFinder is robust to incomplete models, differing gene lengths, and larger phylogenetic
140 distances (Emms and Kelly, 2015). Gene families (orthogroups) in OrthoFinder are defined as
141 homologous genes descended from a single gene from the last common ancestor of the species
142 examined. It is assumed that a parental gene of each orthogroup was present in the common
143 ancestor of the seven species investigated. Three independent runs were conducted with
144 OrthoFinder: Juglans-specific, Juglans with the Pterocarya outgroup, and all species with a set
145 of 6 selected Eurosids (*Citrus grandis, Eucalyptus grandis, Arabidopsis thaliana, Carica papaya,*
146 *Populus trichocarpa* and *Quercus robur*). Rates of gene family evolution were calculated for each
147 orthogroup using the stochastic birth and death rate modeling implemented in CAFE (v4.1) (De
148 Bie *et al.* 2006). Species trees were constructed by applying estimated divergence times from
149 literature detailing rosid phylogeny to the known topology (Magallón *et al.* 2014, Dong *et al.*
150 2017). Large variance in gene copy number between species can lead to inaccurate calculation of
151 birth and death rate parameters, therefore large orthogroups with more than 100 gene models
152 were removed prior to the analyses. Orthogroups represented by a single set of paralogs were

also removed because they are uninformative. Rapidly evolving gene families (orthogroups) were identified using CAFE, which models the rate of gene family evolution while accounting for the uncertainty in size that results from imperfect genome annotation. For each set, the lambda (birth and death rate) parameter was calculated uniformly across the phylogeny. Orthogroups with a large size variance among taxa were selected using a CAFE family-wide P-values <0.05. Those orthogroups with accelerated rates of evolution were selected using branch-specific Viterbi P-values <0.05.

Syntelog Analysis

Genome alignment and analysis of syntenic genes was performed for each *Juglans* genome against *Pterocarya stenoptera* using a CoGE (Lyons and Freeling, 2008) SynMAP2 analysis. Genome alignment was performed using Last. Five genes were used as the minimum number of aligned pairs for DAGchainer (Haas *et al.* 2004). Synonymous (Ks) and non-synonymous (Kn) coding sequence divergence was estimated for syntenic protein coding gene pairs with CodeML (Yang, 2007).

RESULTS

Semi-unsupervised Gene Prediction

Errors introduced from genome annotation often lead to inconsistent gene expression estimates and contribute to the inaccurate characterization of gene space, gene family evolution and timing of whole genome duplications (Vijay *et al.* 2013, Denton *et al.* 2014). A novel approach was applied across all seven genomes described in this study that leveraged RNA-Seq reads generated from tissue-specific libraries of *J. regia* (Table 1). This approach took advantage of the deep sequencing by directly aligning reads to the genome to resolve challenges associated with reliance on error-prone and often fragmented *de novo* assembled transcripts (Hoff *et al.* 2016). The bias introduced by using RNA-Seq reads solely from *J. regia* for the annotation of all genomes was partially mitigated by the semi-supervised training of the gene prediction tool, AUGUSTUS, included in BRAKER. Repeat libraries were generated and subsequently used for masking between roughly 44% and 48% of the genomes prior to read alignment (Table 2; Table S1). The raw reads aligned across the genomes at rates inversely proportional to their phylogenetic distance from *J. regia*. Average alignment rates across *J. regia* transcriptome libraries are displayed as total mapped (concordantly mapped): 87.1% (84.2%) in *J. regia,* 88.3% (78.7%) in *J. sigillata*, 51.8% (49.1%) in *J. cathayensis*, 68.0% (49.0%) in *J. nigra*, 41.0% (38.7%) in *J. microcarpa*, 49.7% (48.0%) in *J. hindsii* and 33.2% (31.2%) in the outgroup, *P. stenoptera*. Initial gene prediction estimates from BRAKER2 ranged from 81,753 (*J. hindsii*) to 133,963 (*P. stenoptera*) (Table S2). Filtering of BRAKER2 models considered completeness (start and stop codon present), isoforms, exon lengths, intron lengths, and splice sites. These considerations provided a reduced set of gene models for each genome: 82,610 in *J. nigra,* 76,847 in *J. hindsii,*

114,573 in *J. microcarpa,* 83,457 in *J. sigillata,* 97,312 in *J. cathayensis*, 84,098 in *J. regia*, and 123,420 in *P. stenoptera* (Table S2).

Functional Annotation Filtering of Gene Models

Functional annotation via sequence similarity search (SSS) and gene family assignment (GFA) provides a form of validation for the proposed models and also assesses their completeness. The reciprocal style search required query and target sequence coverage to pass a set threshold, which helped to eliminate unlikely models and produce final gene models sets: 23,607 models with both SSS result and GFA and 4728 with only GFA (28,335 total) in *J. nigra,* 23822 both and 4842 GFA-only (28,724) in *J. hindsii,* 33,711 both and 7900 GFA-only (41,611 total) in *J. microcarpa,* 22,036 both and 4799 GFA-only (26,835 total) in *J. sigillata,* 27,815 both and 6251 GFA-only (34,066 total) in *J. cathayensis*, 25,420 both and 5206 GFA-only (30,626 total) in *J. regia*, and 35,711 both and 8547 GFA-only (44,318 total) in *P. stenoptera* (Table 2; Table S2). Structural assessment of the genes examined splice sites, exons per gene, CDS lengths, and intron lengths (Table 2) and reported average gene/CDS lengths relative to other angiosperm species. The vast majority (> 98% in all species) of the splice sites were canonical (GT/AG). All other splice site detected were GC/AG variants.

Benchmarking Genome Annotation Completeness

The embryophyta collection of 1440 genes derived from OrthoDB and assessed via BUSCO were compared to the genome assembly and the final gene model sets (Figure 2; Table S3). Across members of *Juglans* genus, we observed (90-95% complete models) estimated in the genome. Following selection of the gene models, we observed 77 to 89% completeness, considering complete models only, and 82.5 to 92% considering also partial models. As expected, *P. stenoptera* reported a lower percentage against the genome but was comparable with *Juglans* at the gene level.

Orthologous Group Construction

Two OrthoFinder runs that differed in adjacent clade inclusivity were used to identify homology relationships between genes of the selected species. One run of annotated Juglandaceae (6 *Juglans*, 1 *Pterocarya*) species, and another including previously annotated genomes from across the Eurosid superorder (13 species). OrthoFinder assigned 216,778 (92.5%) of the 234,455 total genes from the Juglandaceae set to 26,458 orthogroups (Figure 3B, File S1). A total of 161 genes (0.1%) were present in 56 species-specific orthogroups. 14,429 orthogroups contained at least one gene from each species. OrthoFinder analysis of selected Eurosid species assigned 401,186 (92.8.%) of the 456,424 total genes to 22,189 orthogroups (File S2). Of these, a total of 3054 genes (0.7%) were present in 488 species-specific orthogroups and 6722 orthogroups contained at least one gene from each species. Addition of peripheral species

229 across to the set lead to resulted in an average gene contribution per species in orthogroups.
230 This trend is also reflected in the lower number of orthogroups in the larger sets (Table S4). The
231 Juglandaceae set included 1159 genes that formed 538 orthogroups specific to *Juglans* sect.
232 *Dioscaryon* and 1608 genes that formed 437 orthogroups specific to all sampled members of
233 *Juglans* sect. *Rhysocaryon*. Within *Rhysocaryon*, 905 genes formed 389 orthogroups were specific
234 to the tangentially distributed species, *J. microcarpa* and *J. nigra* but not found in the
235 geographically isolated *J. hindsii*. 564 genes formed 149 orthogroups that were specific to the
236 three Eurasian *Juglans* species (*J. regia*, *J. sigillata* and *J. cathayensis*). Finally, 5268 genes from
237 *Juglans* species formed 661 orthogroups that excluded the outgroup, *P. stenoptera*. 2025 (6.6%) of
238 30,626 genes were not assigned to orthogroups in *J. regia*, 2801 (8.2%) of 34,066 in *J. cathayensis*,
239 1138 (4.0%) of 28,664 in *J. hindsii*, 3181 (7.6%) of 41,611 in *J. microcarpa*, 934 (3.3%) of 28,335 in *J.*
240 *nigra*, 1251 (4.7%) of 26,835 in *J. sigillata*, 6347 (14.3%) of 44318 in *P. stenoptera* (Figure 3A; Figure
241 3B)
242
243 *Analysis of Gene Family Evolution*
244 Before CAFE analysis, orthogroups derived from OrthoFinder were filtered to exclude those
245 composed entirely of paralogs and others with > 100 gene copies and resulted in the removal of
246 57 of 26,458 (0.2%) orthogroups from the Juglandaceae set, and 1880 of 22,189 (8.5%)
247 orthogroups from the Eurosids. Calculated lambda values were 0.02396 and 0.02197 for
248 Juglandaceae and Eurosid sets, respectively. The higher lambda in Juglandaceae set
249 corresponds with a higher calculated average rate of gene family evolution of the 460 significant
250 rapidly evolving orthogroups discovered based on the Eurosid set, 153 (+131/-22) had
251 significant changes in *J. microcarpa*, 102 (+57/-45) in *J. regia*, 86 (+62/-24) in *J. cathayensis*, 76 (+30/-
252 46) in *J. sigillata*, 61 (+22/-39) in *J. nigra*, 58 (+32/-26) in *J. hindsii,* and 139 (+113/-24) in *P. stenoptera*
253 (Figure 5, File S4). The Juglandaceae set revealed 430 significant rapidly evolving gene families
254 of which 168 (+123/-45) had significant size changes at the *J. microcarpa* terminal branch, 141
255 (+86/-55) in *J. regia*, 92 (+72/-20) in *J. cathayensis*, 98 (+39/-59) in *J. sigillata*, 101 (+32/-69) in *J. nigra*,
256 77 (+40/-37) in *J. hindsii,* and 98 (+67/-31) in *P. stenoptera* (File S3).
257
258 *Juglans hindsii Gene Family Evolution*
259 In the Juglandaceae comparison, a Heat shock cognate 70 kDa (HSC70) orthogroup
260 (OG0000060) was expanded in both *J. hindsii* (23 genes) and *J. microcarpa* (30 genes) relative to all
261 species outside of *Rhysocaryon* (1-2 genes) and unexpectedly lacked gene models from *J. nigra*.
262 SAPK10-like serine/threonine kinase orthogroup (OG0001146) was also expanded in both *J.*
263 *hindsii* (8 genes) and *J. microcarpa* (7 genes) relative to other species (0-4 genes) and lacked *J.*
264 *nigra* gene models. A probable sugar phosphate/phosphate translocator orthogroup
265 (OG0000474) was expanded in *J. hindsii* (17 genes) relative to other species (0-4 genes). Two
266 putative gene families annotated as Rust resistance kinase Lr10 (OG0000113, OG0000120) were

expanded in both *J. hindsii* (+6, +12) and *J. cathayensis* (+3, +15). OG0000120 expansions were substantial considering other species were present in 0-4 gene models.

Juglandaceae REDUCED WALL ACETYLATION 2 (RWA2) (OG0000145), putative disease resistance protein (OG0000022) and receptor-like protein kinase FERONIA-like (OG0000471) orthogroups lacked *J. hindsii* gene models despite being represented by every other species. In addition to loss in *J. hindsii*, RWA2 was also highly expanded in *J. cathayensis* (23 genes) relative to other species (0-5 genes). Comparative analysis of gene models revealed an absence of *J. hindsii* models across five orthogroups annotated as receptor-like protein kinase FERONIA-like in the Juglandaceae set (OG0000687, OG0000471, OG0022392, OG0009045, OG0013911) including two for which every other species is represented (OG0000687, OG0000471). A Chitinase-3-like protein (Cht3) orthogroup (OG0001222) lacked genes from *J. hindsii* and *J. sigillata* but included multiple genes from every other annotated species. An orthogroup annotated as SENESCENCE-RELATED GENE 1 (SRG1) (OG0000050) was highly contracted in *J. hindsii* (2 genes) relative to other species (8-17 genes). UDP-glycosyltransferase 89B2 orthogroup (OG0000128) lacked *J. hindsii* gene models but contained at least 5 from other annotated species. Two large orthogroups, annotated as Wall-associated receptor kinase 2 (WAK2) (OG0000007, OG0000003) were significantly contracted in *J. hindsii* (2 and 5 genes) and *J.* sigillata (0 and 1 genes). Similarly, another orthogroup annotated as WAK3 (OG0000405), lacked gene models from both *J. hindsii* and *J. sigillata*.

Rhysocaryon Gene Family Evolution

Functional annotation of Juglandaceae orthogroups expanded in *J. microcarpa* revealed high incidence of transferase activity (GO:0016740) which occurred in 8 of 123 orthogroup annotations. An orthogroup annotated as ankyrin repeat-containing (OG0000093) was significantly expanded in both *J. microcarpa* (22 genes) and *J. sigillata* (16 genes) relative to other species (0-6 genes). Three orthogroups annotated as Kinesin-like protein KIN-4C, Phosphatidylinositol 4-kinase gamma 7 (P4KG7) and RNA-dependent RNA polymerase (OG0002363, OG0001584 and OG0013906) were expanded in *J. microcarpa* and *J. nigra* relative to other annotated species. An activating signal cointegrator orthogroup (OG0022144) with a zinc finger-C2HC5 (Pfam:PF06221) domain was expanded (+13) in *J. microcarpa*. OG0000386, annotated as topless-related protein 1 (TPR1) was also expanded (+6). Three orthogroups annotated as "wall-associated receptor kinase-like" (OG0000502, OG0000046 and OG0000685) lacked gene models from both *J. hindsii* and *J. microcarpa*. OG0000685 also lacked *J. sigillata* gene models.

The large Juglandaceae callose synthase 3-like orthogroup (OG0000004) is absent in *J. nigra* and highly contracted in *J. microcarpa* and *J. cathayensis* (7 genes) relative to other species (32-36

genes). Four cyclic nucleotide-gated ion channel orthogroups involved in Plant-pathogen interaction (KEGG:04626), are lost or highly contracted in *J. nigra*: OG0000038 (-7), OG0000567 (-3), OG0000177 (-4), OG0000603 (-2).

Dioscaryon Gene Family Evolution

Gene family expansions specific to *Dioscaryon* include (+3) ABC transporter B family orthogroup (OG0000286), and (+2) Ethanolamine-phosphate (OG0001347) orthogroups. Juglandaceae cationic peroxidase (CEVI16) orthogroup (OG0000173) related to Phenylpropanoid biosynthesis (GO:0009699) is contracted in *Juglans* sect. *Dioscaryon*. Probable reticuline oxidase families (OG0000562, OG0000531) annotated as containing BBE (Pfam:PF08031) and FAD binding 4 (Pfam:PF1565) lack *Dioscaryon* gene models while all non-*Dioscaryon* species contribute at least 3 gene copies in each orthogroup. *Dioscaryon* gene models were absent in nodulin-like orthogroup (OG0000206) (-3 genes). Contractions in F-box protein orthoroup (OG0000054) and Oxygen-evolving enhancer protein 2 (OG0000122) were also observed (-4 and -3 genes, respectively). Two SWIM zinc finger orthogroups (OG0000266, OG0000510) lack gene models from *J. regia*, *J. sigillata* and *J. microcarpa*.

Gene family expansions in *J. regia* include (+4) 26s proteasome regulatory subunit (OG0019963), (+3) thaumatin-like protein (OG0000263), (+4) STOMATAL CYTOKINESIS DEFECTIVE 1-like (OG0001205), (+3) mitogen-activated protein kinase kinase kinase (OG0012715), (+4) Hydroxyproline O-galactosyltransferase GALT6 (OG0004422), (+10) tubulin beta-6 chain (OG0000238). Expanded orthogroups in *J. sigillata* include (+11) endoribonuclease dicer (OG0000131).

Divergence Estimates

We estimated the distribution of nucleotide substitution rates at silent codon positions between each of the *Juglans* genomes studied and the outgroup *Pterocarya stenoptera*. For each pairwise analysis, we observed similar bimodal distributions of synonymous substitution rates (Ks) between syntenic blocks of genes (Figure 4a). For these syntenic blocks of genes, a whole genome duplication event would give rise to such a bimodal distribution in time to the most recent common ancestor. For each species pair, we thus estimated the two modes of the distribution (Table S5). The estimates for the higher mode ranged from a low of Ks = 0.356 to a high of Ks = 0.364 with an average value of Ks = 0.361. The lower mode ranged from a low of Ks = 0.050 to a high of Ks = 0.054 with an average value of Ks = 0.053. While the non-synonymous substitution rates (Kn) between syntenic blocks of genes were much lower, the distributions were also bi-modal in appearance (Figure 4b)

342 The annotation of the genome of *Quercus robur* (oakgenome.fr) allowed us to perform the same
343 analysis with a species whose common ancestor predates the whole genome duplication event.
344 We chose the genomes of *J. regia* and *P. stenoptera* as the best representatives of their genera. In
345 both cases, while the histogram was much sparser due to the additional divergence, a single
346 prominent peak was observed. For *J. regia* against *Q. robur*, it was observed at a value of Ks =
347 0.49 and for *P. stenoptera* against *Q. robur,* it was observed at a value of Ks = 0.53. These
348 divergence estimates are greater than all values estimated in the *Juglans-Pterocarya* comparisons.
349
350 **DISCUSSION**
351 In this study, we utilized a comprehensive *J. regia* transcriptome dataset to produce high-quality
352 genome annotations of six recently assembled species within *Juglans* and a single member of the
353 sister genus, *Pterocarya*. The gene model set completeness as measured by BUSCO (82-92%)
354 suggests our annotation pipeline is suitable for wide capture of protein-coding genes. Although
355 the gene prediction software, BRAKER2 seems to return far fewer false positive gene models
356 than its predecessor BRAKER, the process of removing the extraneous models remains essential
357 to producing genome annotations that can be leveraged by the community. The gene model
358 filtration steps presented here handle multiexonic and monoexonic genes separately and
359 examine both structural and functional qualities of models to permit only those of the highest
360 confidence. This set of diploid genome annotations is the most comprehensive to date for any
361 hardwood genus and represents an invaluable resource for comparative genomics studies
362 within *Juglans* and for other clades (Tuskan *et al.* 2018).
363
364 The annotated species represent each of the three sections of *Juglans* (*Cardiocaryon*, *Juglans* (syn.
365 *Dioscaryon*) and *Rhysocaryon*) constituting a broad depiction of the diversity in the genus. These
366 annotations will serve as a platform for identifying genetic underpinnings of high-value
367 agricultural characteristics such as drought tolerance and disease resistance that are scattered
368 across the various species (Bernard *et al*. 2018). Moreover, they have the potential to add a new
369 dimension to the ongoing medicinal natural products search within *Juglans* (Yao *et al.* 2012; Xu
370 *et al.* 2013; Kim *et al.* 2018).
371
372 *Gene Family Size Evolution*
373 There was no considerable asymmetry between the major functional categories assigned to
374 rapidly expanding and contracting gene families across Juglandaceae. Of the 333 instances of
375 gene family contraction calculated across the Juglandaceae set, the most frequent Gene
376 Ontology molecular function annotations were 26 transferase activity (GO:0016740), 9 lyase
377 activity (GO:0016829), 9 cyclase activity (GO:0009975). High occurrence EggNOG descriptions
378 of contracting orthogroups included 25 that contained "resistance", 54 that contained "kinase",
379 8 "cytochrome P450" and 7 "channel". For 428 instances of gene family expansion, the most

frequent molecular function annotations were 29 transferase activity (GO:0016740), 8 transmembrane transporter activity (GO:0022857) and 7 heterocyclic compound binding (GO:1901363). High occurrence EggNOG descriptions of expanding orthogroups include 51 containing "kinase", 19 that contained "resistance" 17 that contained "synthase". Comparisons of annotated rapidly evolving gene families between species did reveal disproportionate gains and losses. *J. microcarpa*, for example has 7 instances of expansion in "synthase" orthogroups while *J. sigillata* has 0 and *J. hindsii* demonstrates contraction of 10 "kinase" orthogroups, while only 2 such contractions were calculated in *J. cathayensis* (0 at preceding node shared with *Dioscaryon*). These divergent patterns of gene family evolution underline the importance of having comprehensive genetic resources for multiple species within a single clade. The 6 *Juglans* genome annotations provide an immediate reference for one another and construct a genetic background for the genus.

Of the 153 significant gene family size changes in *J. microcarpa*, 131 represent expansions, while the changes in other *Juglans* species are more evenly distributed between expansions and contractions. Inflated number of significant expansions in *J. microcarpa* could be reflective of uncollapsed heterozygosity left behind by the genome assembly process, especially given the unexpectedly large size of the *J. microcarpa* assembly. A similar, but less pronounced pattern is observed in *J. cathayensis*.

Loss of Reticuline Oxidase in Dioscaryon

The absence of *Dioscaryon* gene models in the reticuline oxidase (berberine bridge enzyme, BBE) annotated orthogroups suggests a contraction before their divergence 22 MYA. Enzymes in this family have been shown to contribute to alkaloid production (Fujii *et al.* 2007) in California poppy (*Eschscholzia californica*) and have been implicated in monolignol metabolism. Extreme (400-fold) upregulation of enzymes in this family has been observed during pathogen attack and osmotic stress in *Arabidopsis* (Daniel *et al.* 2015). Recent work in *Arabidopsis* demonstrated the function of one BBE-like enzyme in oxidizing oligogalacturonides (OGs) and thereby diminishing their elicitor activity (Benedetti *et al.* 2018). Because *J. regia* and *J. sigillata* are considered domesticated and semi-domesticated species, respectively, it remains within the realm of possibility that the loss of the BBE gene family is an aspect of their domestication syndromes, where loss of chemical protection against herbivores is artificially selected. On the contrary, the most parsimonious conclusion is that the loss occurred in the *Dioscaryon* ancestor instead of being the result parallel evolution though independent domestications. This scenario does not rule out the idea that these species were favored for their tamed secondary metabolite profiles. Until recently, chemical analyses in *Juglans* have been limited to observational studies and comparisons of different cultivars within a species (Vu *et al.* 2018; Vu *et al.* 2019). Additional studies contrasting metabolomic profiles of domesticated species with their wild relatives will

418 offer valuable insight into tree domestication, especially when paired with genome annotations.
419
420 *Disease Resistance*
421 In California, the cultivation of *J. regia* is most commonly facilitated through the use of Paradox
422 rootstock (*J. hindsii* ♂ x *J. regia* ♂), which is valued for its resistance to soil-borne pathogens
423 (Browne *et al*. 2015, Potter *et al.* 2002). Despite higher resistance to several diseases, Paradox
424 rootstock remain susceptible to *Armillaria* root rot, which is caused by a basidiomycete, *A. mellea*
425 in California (Baumgartner *et al.* 2013). The impact of this disease is worsened by the lack of
426 post-infection controls. Accordingly, discovering resistant Paradox hybrids has been the focus
427 of some research, but has achieved limited success relative to the levels of *Armillaria* resistance
428 reported in *J. hindsii* (Drakulic *et al*. 2017).
429
430 Interactions between *Arabidopsis* and the fungal pathogen, *Fusarium oxysporum* are intensely
431 studied as a model for plant fungal diseases. In this system, *F. oxysporum* infections are
432 potentiated by the alkalinization of soil around host root tissue caused by the stimulation of
433 plant RALF-triggered alkalinization response by pathogen secreted RALF (Rapid Alkalinization
434 Factor) homologs (Masachis *et al.* 2016). These fungal peptides target various members of
435 transmembrane receptor-like kinases encoded by the plant *Catharanthus roseus* Receptor-like
436 Kinase (CrRLK1L) gene family. There are 17 reported CrRLK1L protein orthologs in *Arabidopsis*
437 that have been implicated in a variety of processes including immunity signalling, abiotic stress
438 response and cell wall dynamics (Kessler *et al.* 2010, Richter *et al.* 2017, Guo *et al.* 2018, Richter *et*
439 *al.* 2018). A number of Basidiomycetes genomes have been reported to encode RALF homologs,
440 making it plausible that *Armillaria* is among the fungi that utilize RALF-homolog effectors in
441 infection.
442
443 The current literature suggests a central role for CrRLK1L with respect to *F. oxysporum*
444 resistance. It is possible that the reduction or absence of the CrRLK1L orthologs (annotated as
445 FERONIA) in *J. hindsii* is correlated with its increased resistance to *A. mellea* infection like to *F.*
446 *oxysporum*. If the gene family is lost in *J. hindsii*, discovering any compensatory mechanisms that
447 might maintain the integrity of CrRLK1L-involved pathways could have application in
448 engineering fungal-resistant plants.
449
450 Similar to the observations made of FERONIA knockouts, loss of function *Arabidopsis*
451 mutations in RWA2 (reduced wall acetylation-2) led to increased resistance against the
452 Ascomycete pathogen, *Botrytis cinerea*, the causal agent of grey mold (Manabe *et al.* 2011). *B.*
453 *cinerea* belongs to a family of fungi, Botryosphaeriaceae, several of which are known to infect
454 the nuts of *J. regia* and related species (Moral et al. 2010). The Juglandaceae RWA2 orthogroup
455 was missing in *J. hindsii* gene models. RWA2 is involved in secondary cell wall synthesis and is

regulated by SND1 (Lee *et al.* 2011). No experiments to date have assessed the susceptibility of various *Juglans* species to *B. cinerea*, but it would be interesting to test for resistance to the pathogen in a species without RWA2. Loss of Chitinase-3 (Cht3) in *J. hindsii* is consistent with the loss of FERONIA and RWA2. Cht3 (along with glucanase and thaumatin-like protein) are aspects of plant response to fungal invasion (Singh *et al.* 2012). If the loss of FERONIA and RWA2 do correspond to a weakened compatible host signature, the decreased incidence of fungal infection would render such defense responses inessential.

The wall-associated kinases (WAKs) are a family of transmembrane receptor-like proteins that bind pectin in the extracellular matrix (ECM) (Wagner and Kohorn, 2001). They are necessary for cell expansion in *Arabidopsis* seedlings, but when bound to OGs also function in defense response through Enhanced disease susceptibility 1 (EDS1) and Phytoalexin deficient 4 (PAD4) dependent activation of MPK6-dependent pathway (Kohorn *et al*. 2009; Brutus *et al*. 2010; Kohorn *et al.* 2014; Davidsson *et al.* 2017). Recent studies of WAKs have shed light on their role in plant response to abiotic stressors (Marakli and Gozukirmizi. 2018, Xia *et al*. 2018) but many WAK family genes remain without functional characterization. Because of this, the parallel contraction and loss of *J. hindsii* and *J. sigillata* genes from multiple WAK annotated orthogroups is difficult to speculate on. A more elaborate depiction of the WAK gene family will certainly shed light on the significance of these losses. It is interesting to note, however, that two gene families (WAK and BBE) which have members known to interact with OGs are both contracted in *J. sigillata*. These losses suggest a significant shift in *J. sigillata* effector-triggered immunity.

Insights into Phenology

Given the pronounced levels of local adaptation observed in forest trees (Eckert *et al.* 2015, Pina-Martins *et al.* 2018) along with the recent and dramatic shifts in climate, it will be crucial to continue to study the resilience of the existing cultivars. These observations can be associated with the genomic profiles of affected species such that differential response can be better understood. Monitoring some cultivars has provided data about climate change-induced phenology shifts in *Juglans* that vary across genotype (Pope *et al.* 2012). In *J. regia* cultivars, variation in ecodormancy and cold deacclimation leading to budbreak are strongly correlated with genotype, but the genes responsible for the differences have not been resolved (Charrier *et al.* 2011). Phenological variation also exists across the genus, for example, *J. hindsii* is known to have a delayed leaf-out and leaf drop relative to the other *Rhysocaryon* species, *J. californica* (Mcgranahan *et al.* 1988). Understanding this variation has applications in both agricultural practices and conservation.

The contraction of an SRG1 annotated gene family in *J. hindsii* could be related to phenology differences. The abscisic acid (ABA) and ethylene induced (Sui *et al*. 2015) zinc-finger

transcription factor, SRG1 has been implicated in leaf senescence in *Arabidopsis* (Callard *et al.* 1996, Cui *et al.* 2018) and fruit ripening in strawberry (Chen *et al*. 2016). Discovering additional contractions (and expansions) in phenology-related gene families between closely related species might set a natural experiment for establishing the genetic signatures correlated with species susceptible to climate change-associated fitness loss.

Mutation rate estimates and evidence of WGD

We observed similar bimodal distributions of Ks values among syntenic blocks of genes in each of the *Juglans-Pterocarya* pairwise analyses (Figure 4A). The bimodal distribution can be attributed to a mixture of estimates from two distinct lineages; comparisons between orthologous genes; and comparisons between more distant paralogous genes arising from the whole genome duplication. Bimodal distributions for all *Juglans-Pterocarya* pairwise comparisons are consistent with the WGD occurring at or prior to the radiation of Juglandaceae (Luo et al. 2015). As additional confirmation, the most prominent feature in the same analysis against the annotated genome of *Quercus robur* is a peak at divergence values greater than those estimated for the WGD (Table S5).

Using the larger mode for each of the distributions, we can estimate the nucleotide substitution rate using the same method of Luo *et al.* (2015) for comparison. Similarly, using 60 MYA as the date of the WGD supported by fossil records, we obtain a mutation rate of 3.0x10-9. This rate is higher than their rate of 2.3x10-9 estimated using 14 genes, but consistent with the rates of other woody perennials (e.g. Palm (Gaut *et al.* 1996) and *P. trichocarpa* (Tuskan *et al.* 2006)), and still five times slower than the rate reported for *Arabidopsis* (Koch *et al.* 2000).

A surprising observation was the distance between the two modes. We assume that the estimated Ks of the smaller mode represents the between species divergence. The ratios of the larger to smaller modes ranged from 6.5 to 7.3. This discrepancy with the fossil record (Manchester 1987) may be due to the non-neutral nature of these substitutions and departure from a molecular clock. A relevant observation was recently made using a coalescent based approach. Bai *et al.* (2018) noted that the effective population sizes in their study converged 1.0 MYA. They proposed that this could reflecting the time when the walnut genus last shared a common ancestor, much more recent that previous studies have suggested.

The resources and services provided by *Juglans* have been nutritionally and culturally significant. Their hardwood, used to construct furnishing and musical instruments, is valued among woodworkers. Ink from walnut husks was used by Leonardo da Vinci and Rembrandt. Brown dye from walnut stained fabrics used in classical Rome, medieval Europe, Byzantium and Ottoman. The genus is elevated in poetry across the globe, including for their non-

monetary benefits in Mary Oliver's "The Black Walnut Tree" (Oliver, 1992) and nutritional properties in Tatsuji Miuoshi's "In Praise of a Walnut" (Miuoshi, 1946). We are enthusiastic to contribute to the understanding of and appreciation for this genus by constructing these genome annotation resources.

Data Availability: The genomic resources described here are available at NCBI under BioProject PRJNA445704 and the transcriptomic resources under BioProject PRJNA232394. These resources are also accessible from hardwoodgenomics.org and treegenesdb.org. Functional annotations, gene models and gene transfer format (gtf) files are also available on treegenesdb.org. Scripts and detailed processes used for this study are accessible on https://gitlab.com/tree-genome-annotation/Walnut_Annotation.

Acknowledgements: This project was supported by the California Walnut Board, USDA NIFA SCRI-Award no. 2012-51181-20027 and USDA ARS CRIS project no. 5306-22000-015-00D. We thank the Institute for Systems Genomics Computational Biology Core for access to software and hardware support and Uzay Sezen for providing enthusiasm and suggested revisions.

Table 1:Genome assembly statistics for seven Juglandaceae species

	Juglans. hindsii	*Juglans nigra*	*Juglans cathayensis*	*Juglans microcarpa*	*Juglans sigillata*	*Juglans regia*	*Pterocarya stenoptera*
Assembly							
Version	1.0	1.0	1.0	1.0	1.0	1.1	1.0
Size (Mbp)	605.70	605.05	751.37	896.45	622.24	686.52	936.89
Scaffolds	273,094	232,579	332,634	329,873	282,224	186,636	396,056
N50 (Kbp)	512.79	118.45	158.25	145.01	218.35	278.29	159.70
Annotated Assembly (> 3Kbp scaffolds)							
Size (Mbp)	586.05	580.70	719.60	862.79	585.63	686.52	902.23
Scaffolds	4,672	5,896	10,342	12,024	6,413	11,848	11,574
N50 (Kbp)	540.03	271.37	168.53	151.91	238.36	278.30	167.10

Table 2: Structural and functional annotations for seven Juglandaceae species

	Juglans. hindsii	*Juglans nigra*	*Juglans cathayensis*	*Juglans microcarpa*	*Juglans sigillata*	*Juglans regia*	*Pterocarya stenoptera*
Structural Annotation							
Repeat Content	46.97%	47.34%	48.03%	46.87%	46.69%	47.96%	43.89%
Total Genes	28,664	28,335	34,066	41,611	26,835	30,626	44,318

Total Complete, Multi-exonics	24,500	23,290	28,915	35,319	22,898	26,166	36,984
Total Complete, mono-exons	4,164	4,426	5,151	6,292	3,937	4,460	7,334
Gene Length (Avg)	4,406.38	4,301.45	4,193.80	4,008.01	4,373.40	4,235.02	3,944.81
CDS Length (Avg)	1,267.37	1,277.62	1,220.28	1,199.12	1,250.97	1,220.42	1203.44
Exons per Gene (Average)	6.30	6.38	6.06	5.98	6.32	6.14	5.91
Canonical Splice Sites (%)	98.70%	98.67%	98.69%	98.70%	98.60%	98.77%	98.76%
Functional Annotation							
EnTAP (Similarity Search)	23,822	23,607	27,815	33,711	22,036	25,420	35,771
EnTAP (Gene Family only)	4,842	4,728	6,251	7,900	4,799	5,206	8.547

Figure 1:

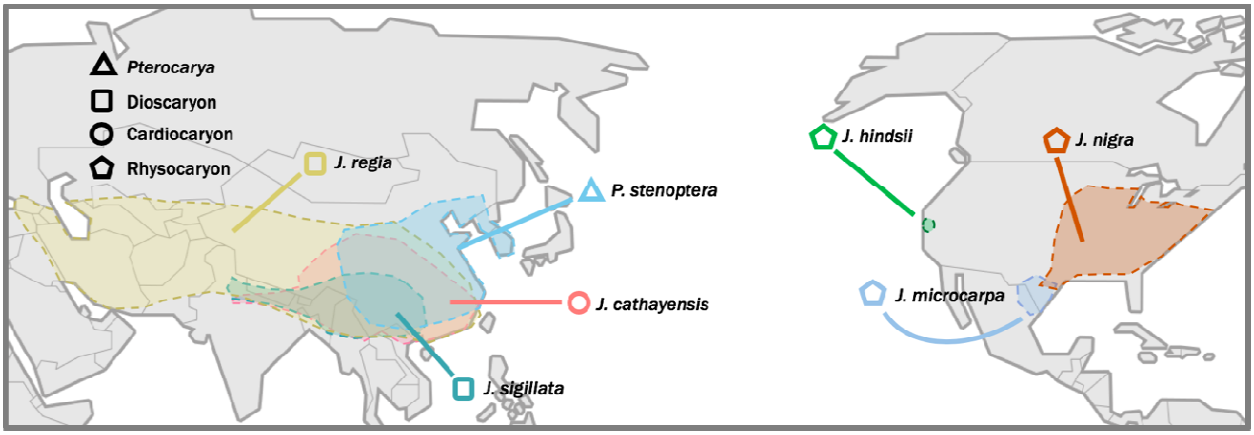

Figure 2:

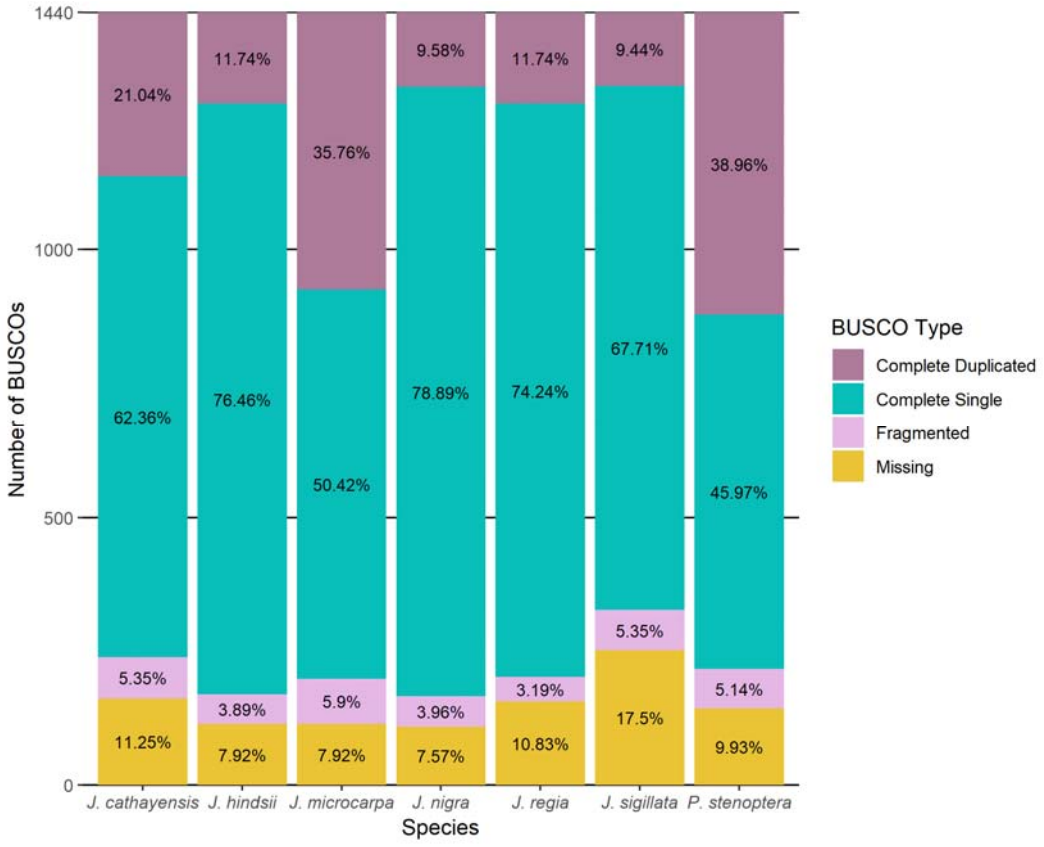
1440
1000
500
0
Number of BUSCOs
21.04%
62.36%
5.35%
11.25%
11.74%
76.46%
3.89%
7.92%
35.76%
50.42%
5.9%
7.92%
9.58%
78.89%
3.96%
7.57%
11.74%
74.24%
3.19%
10.83%
9.44%
67.71%
5.35%
17.5%
38.96%
45.97%
5.14%
9.93%
J. cathayensis
J. hindsii
J. microcarpa
J. nigra
J. regia
J. sigillata
P. stenoptera
Species
BUSCO Type
Complete Duplicated
Complete Single
Fragmented
Missing

Figure 3A/3B:

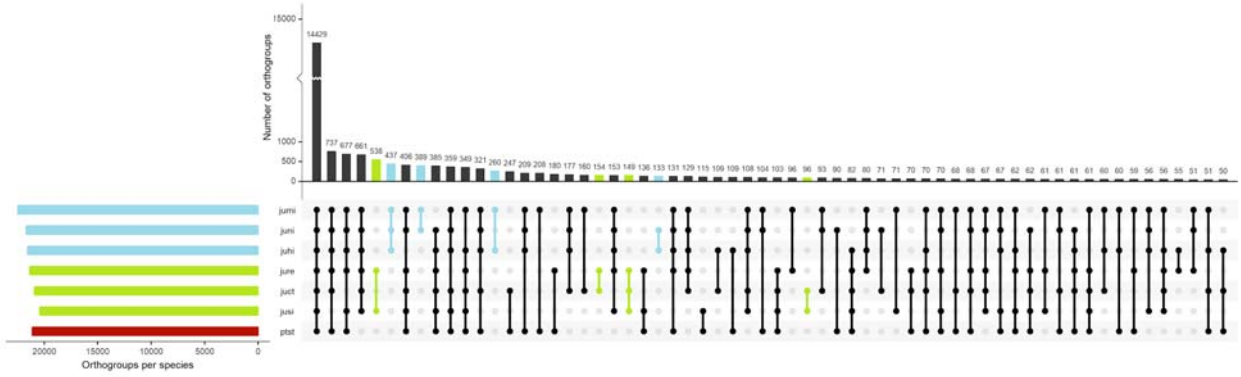
Number of orthogroups
Orthogroups per species
jumi
juni
juhi
jure
juct
jusi
ptst

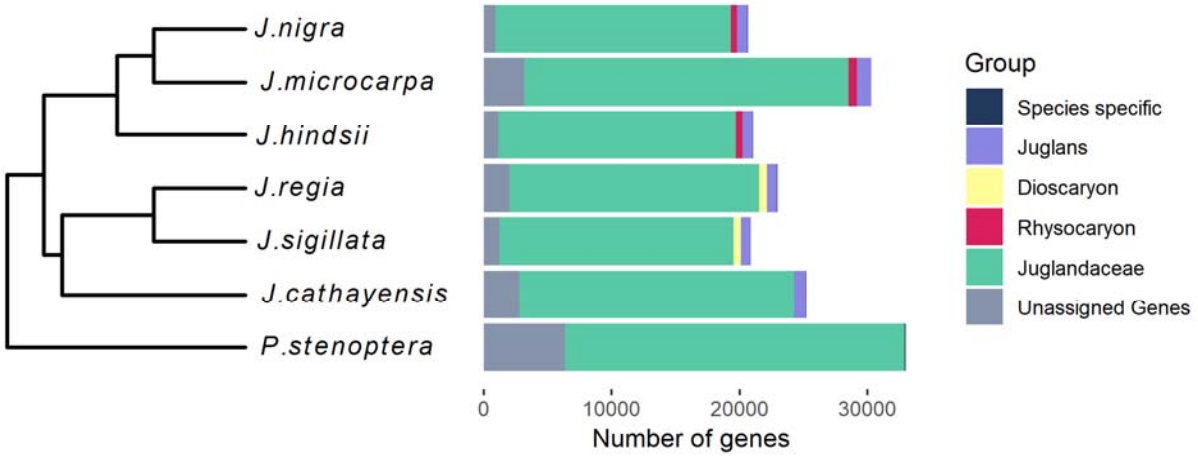
J.nigra
J.microcarpa
J.hindsii
J.regia
J.sigillata
J.cathayensis
P.stenoptera
0
10000
20000
30000
Number of genes
Group
Species specific
Juglans
Dioscaryon
Rhysocaryon
Juglandaceae
Unassigned Genes

Figure 4A/B:

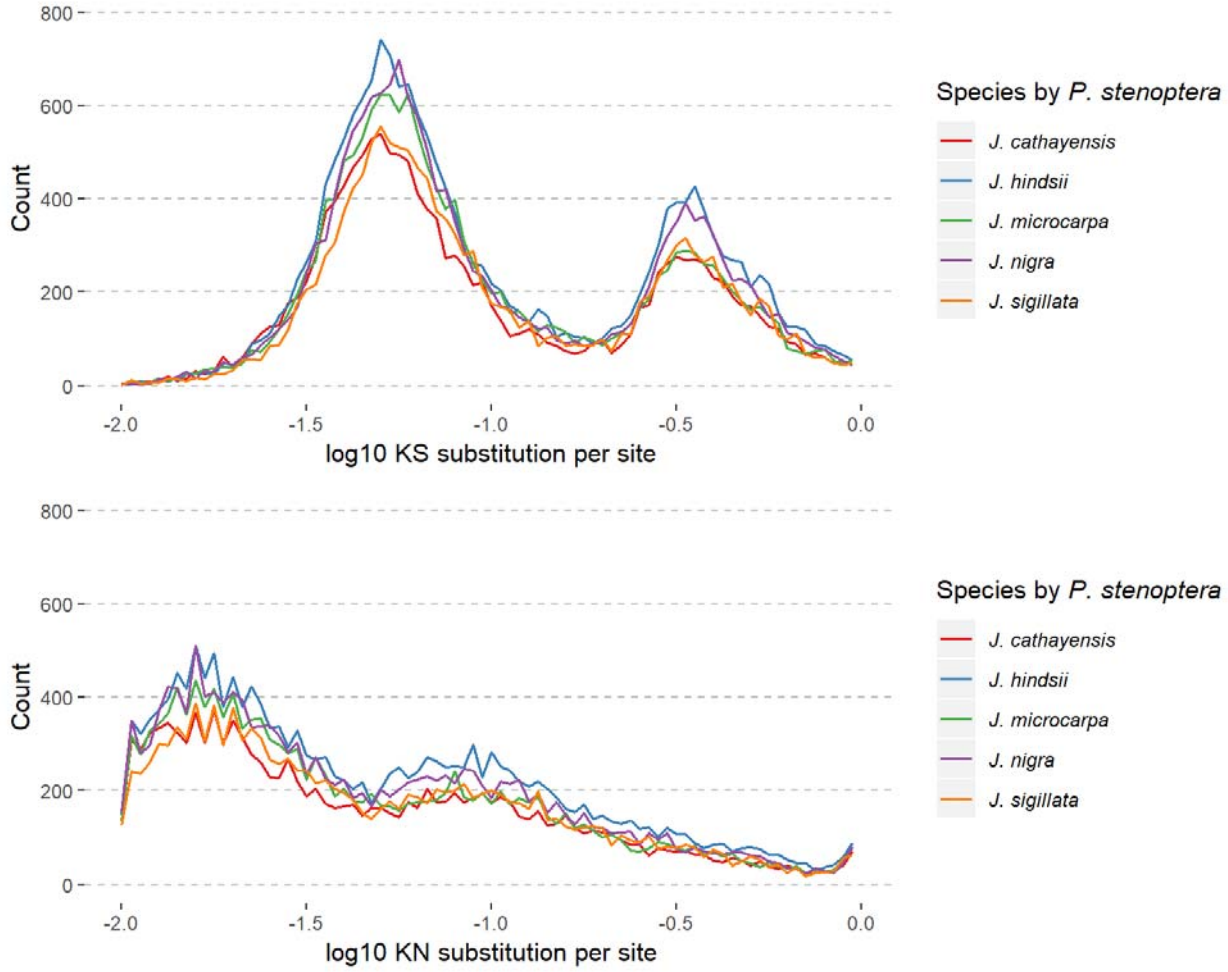
800
600
400
200
0
Count
-2.0
-1.5
-1.0
-0.5
0.0
log10 KS substitution per site
Species by P. stenoptera
J. cathayensis
J. hindsii
J. microcarpa
J. nigra
J. sigillata
800
600
400
200
0
Count
-2.0
-1.5
-1.0
-0.5
0.0
log10 KN substitution per site
Species by P. stenoptera
J. cathayensis
J. hindsii
J. microcarpa
J. nigra
J. sigillata

Figure 5:

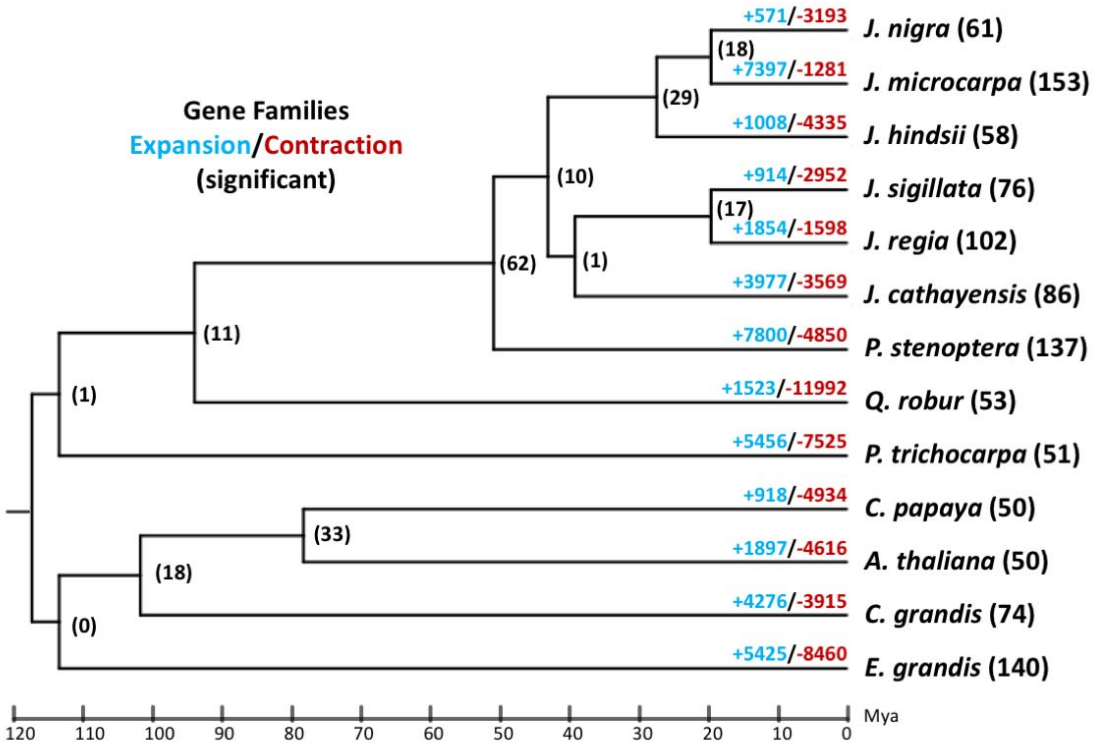

Figure Legends:

Figure 1: Approximate ranges of each annotated species with shapes denoting the three sections of *Juglans* and to the outgroup genus, *Pterocarya.*

Figure 2: As a measure of gene annotation, the gene models from the seven annotations were compared to 30 embryophyta species using BUSCO (Benchmarking Universal Single-copy Orthologs) version 3 (Table S3). The 1,440 universal single-copy orthologs in Embryophyta *odb9* dataset were found either once in the genome (Complete Single), multiple times in the genome (Complete Duplicated), in more than one piece (Fragmented), or were not found at all (Missing).

Figure 3 (A) Distribution of species representation combinations across orthogroups. Tiling beneath the histogram indicates the species contributing gene models to each orthogroup in the set. Set size is displayed as height on histogram. The horizontal histogram indicates the number of orthogroups found in each species. Blue indicates data from groups composed of *Rhysocaryon*

species while green bars show Eurasian species (*Dioscaryon* and *Cardiocaryon*). B) Cladogram with associated stacked histogram reflecting the number of genes belonging to orthogroups specific to the color-indicated groups.

Figure 4 WGD (multi-panel - CoGE+) Histograms of substitution rates for coding genes determined by SynMAP to be syntenic between *Juglans hindsii* and *Pterocarya stenoptera*. Two peaks are visible in both the non-synonymous (A) and synonymous (B) distributions. In both cases the highlighted righthand peak represents the older WGD. Figure S5 summarizes the distributions for all annotated *Juglans* genomes described here against *P. stenoptera*.

Figure 5: Phylogenetic tree constructed from divergence times in literature displaying numbers of expanded (blue) and contracted (red) orthogroups per terminal branch (OrthoFinder Eurosid set) discovered using CAFE. The number of significant (p-value <0.05, viterbi p-value <0.05) expansions and contractions at each node and leaf are shown in parentheses.

Ashburner, M., Ball, C.A., Blake, J.A., et al. (2000) Gene ontology: tool for the unification of biology. The Gene Ontology Consortium. *Nat. Genet.*, **25**, 25–29.

Bai, W.-N., Zeng, Y.-F. and Zhang, D.-Y. (2007) Mating patterns and pollen dispersal in a heterodichogamous tree, Juglans mandshurica (Juglandaceae). *New Phytologist*, **176**, 699–707.

Benedetti, M., Verrascina, I., Pontiggia, D., Locci, F., Mattei, B., Lorenzo, G.D. and Cervone, F. (2018) Four Arabidopsis berberine bridge enzyme-like proteins are specific oxidases that inactivate the elicitor-active oligogalacturonides. *The Plant Journal*, **94**, 260–273.

Bernard, A., Lheureux, F. and Dirlewanger, E. (2017) Walnut: past and future of genetic improvement. *Tree Genetics & Genomes*, **14**, 1.

Browne, G.T., Grant, J.A., Schmidt, L.S., Leslie, C.A. and McGranahan, G.H. (2011) Resistance to Phytophthora and Graft Compatibility with Persian Walnut among Selections of Chinese Wingnut. *HortScience*, **46**, 371–376.

Brutus, A., Sicilia, F., Macone, A., Cervone, F. and Lorenzo, G.D. (2010) A domain swap approach reveals a role of the plant wall-associated kinase 1 (WAK1) as a receptor of oligogalacturonides. *PNAS*, **107**, 9452–9457.

Buzo, T., McKenna, J., Kaku, S., Anwar, S.A. and McKenry, M.V. (2009) VX211, A Vigorous New Walnut Hybrid Clone with Nematode Tolerance and a Useful Resistance Mechanism. *J Nematol*, **41**, 211–216.

Callard, D., Axelos, M. and Mazzolini, L. (1996) Novel Molecular Markers for Late Phases of the Growth Cycle of Arabidopsis thaliana Cell-Suspension Cultures Are Expressed during Organ Senescence. *Plant Physiology*, **112**, 705–715.

Chakraborty, S., Britton, M., Wegrzyn, J., et al. (2015) YeATS - a tool suite for analyzing RNA-seq derived transcriptome identifies a highly transcribed putative extensin in heartwood/sapwood transition zone in black walnut. *F1000Res*, **4**.

Chen, J., Mao, L., Lu, W., Ying, T. and Luo, Z. (2016) Transcriptome profiling of postharvest strawberry fruit in response to exogenous auxin and abscisic acid. *Planta*, **243**, 183–197.

Cheng, C.-Y., Krishnakumar, V., Chan, A.P., Thibaud-Nissen, F., Schobel, S. and Town, C.D. (2017) Araport11: a complete reannotation of the Arabidopsis thaliana reference genome. *Plant J.*, **89**, 789–804.

Cui, B., Pan, Q., Clarke, D., Villarreal, M.O., Umbreen, S., Yuan, B., Shan, W., Jiang, J. and Loake, G.J. (2018) S -nitrosylation of the zinc finger protein SRG1 regulates plant immunity. *Nature Communications*, **9**, 4226.

Daniel, B., Pavkov-Keller, T., Steiner, B., et al. (2015) Oxidation of Monolignols by Members of the Berberine Bridge Enzyme Family Suggests a Role in Plant Cell Wall Metabolism. *J. Biol. Chem.*, **290**, 18770–18781.

Davidsson, P., Broberg, M., Kariola, T., Sipari, N., Pirhonen, M. and Palva, E.T. (2017) Short oligogalacturonides induce pathogen resistance-associated gene expression in Arabidopsis thaliana. *BMC Plant Biol*, **17**.

De Bie, T., Cristianini, N., Demuth, J.P. and Hahn, M.W. (2006) CAFE: a computational tool for the study of gene family evolution. *Bioinformatics*, **22**, 1269–1271.

Denton, J.F., Lugo-Martinez, J., Tucker, A.E., Schrider, D.R., Warren, W.C. and Hahn, M.W. (2014) Extensive Error in the Number of Genes Inferred from Draft Genome Assemblies. *PLOS Computational Biology*, **10**, e1003998.

Dong, W., Xu, C., Li, W., Xie, X., Lu, Y., Liu, Y., Jin, X. and Suo, Z. (2017) Phylogenetic Resolution in Juglans Based on Complete Chloroplast Genomes and Nuclear DNA Sequences. *Front. Plant Sci.*, **8**.

Drakulic, J., Gorton, C., Perez-Sierra, A., Clover, G. and Beal, L. (2017) Associations Between Armillaria Species and Host Plants in U.K. Gardens. *Plant Disease*, **101**, 1903–1909.

Eckert, A.J., Maloney, P.E., Vogler, D.R., Jensen, C.E., Mix, A.D. and Neale, D.B. (2015) Local adaptation at fine spatial scales: an example from sugar pine (Pinus lambertiana, Pinaceae). *Tree Genetics & Genomes*, **11**, 42.

Emms, D.M. and Kelly, S. (2015) OrthoFinder: solving fundamental biases in whole genome comparisons dramatically improves orthogroup inference accuracy. *Genome Biology*, **16**, 157.

Famula, R.A., Richards, J.H., Famula, T.R. and Neale, D.B. (2018) Association genetics of carbon isotope discrimination and leaf morphology in a breeding population of Juglans regia L. *Tree Genetics & Genomes*, **15**, 6.

Finn, R.D., Bateman, A., Clements, J., et al. (2014) Pfam: the protein families database. *Nucleic Acids Res*, **42**, D222–D230.

Fujii, N., Inui, T., Iwasa, K., Morishige, T. and Sato, F. (2007) Knockdown of berberine bridge enzyme by RNAi accumulates (S)-reticuline and activates a silent pathway in cultured California poppy cells. *Transgenic Res*, **16**, 363–375.

Gaut, B.S., Morton, B.R., McCaig, B.C. and Clegg, M.T. (1996) Substitution rate comparisons between grasses and palms: synonymous rate differences at the nuclear gene Adh parallel rate differences at the plastid gene rbcL. *PNAS*, **93**, 10274–10279.

Guo, H., Nolan, T.M., Song, G., Liu, S., Xie, Z., Chen, J., Schnable, P.S., Walley, J.W. and Yin, Y. (2018) FERONIA Receptor Kinase Contributes to Plant Immunity by Suppressing Jasmonic Acid Signaling in Arabidopsis thaliana. *Current Biology*, **28**, 3316-3324.e6.

Haas, B.J., Delcher, A.L., Wortman, J.R. and Salzberg, S.L. (2004) DAGchainer: a tool for mining segmental genome duplications and synteny. *Bioinformatics*, **20**, 3643–3646.

Hart, A.J., Ginzburg, S., Xu, M. (Sam), Fisher, C.R., Rahmatpour, N., Mitton, J.B., Paul, R. and Wegrzyn, J.L. (2018) EnTAP: Bringing Faster and Smarter Functional Annotation to Non-Model Eukaryotic Transcriptomes. *bioRxiv*, 307868.

Hoff, K.J., Lange, S., Lomsadze, A., Borodovsky, M. and Stanke, M. (2016) BRAKER1: Unsupervised RNA-Seq-Based Genome Annotation with GeneMark-ET and AUGUSTUS. *Bioinformatics*, **32**, 767–769.

Jensen, L.J., Julien, P., Kuhn, M., Mering, C. von, Muller, J., Doerks, T. and Bork, P. (2008) eggNOG: automated construction and annotation of orthologous groups of genes. *Nucleic Acids Res*, **36**, D250–D254.

Kessler, S.A., Shimosato-Asano, H., Keinath, N.F., Wuest, S.E., Ingram, G., Panstruga, R. and Grossniklaus, U. (2010) Conserved Molecular Components for Pollen Tube Reception and Fungal Invasion. *Science*, **330**, 968–971.

Kim, D., Pertea, G., Trapnell, C., Pimentel, H., Kelley, R. and Salzberg, S.L. (2013) TopHat2: accurate alignment of transcriptomes in the presence of insertions, deletions and gene fusions. *Genome Biol.*, **14**, R36.

Kim, S.-H., Lee, K.-S., Son, J.-K., Je, G.-H., Lee, J.-S., Lee, C.-H. and Cheong, C.-J. (1998) Cytotoxic Compounds from the Roots of Juglans mandshurica. *J. Nat. Prod.*, **61**, 643–645.

Koch, M.A., Haubold, B. and Mitchell-Olds, T. (2000) Comparative Evolutionary Analysis of Chalcone Synthase and Alcohol Dehydrogenase Loci in Arabidopsis, Arabis, and Related Genera (Brassicaceae). *Mol Biol Evol*, **17**, 1483–1498.

Kohorn, B.D., Johansen, S., Shishido, A., Todorova, T., Martinez, R., Defeo, E. and Obregon, P. (2009) Pectin activation of MAP kinase and gene expression is WAK2 dependent. *The Plant Journal*, **60**, 974–982.

Kohorn, B.D., Kohorn, S.L., Saba, N.J. and Meco-Martinez, V. (2014) Requirement for Pectin Methyl Esterase and Preference for Fragmented Over Native Pectins for Wall Associated Kinase Activated, EDS1/PAD4 Dependent Stress Response in Arabidopsis. *J. Biol. Chem.*, jbc.M114.567545.

Lee, C., Teng, Q., Zhong, R. and Ye, Z.-H. Four Arabidopsis REDUCED WALL ACETYLATION Genes are Expressed in Secondary Wall-Containing Cells and Required for the Acetylation of Xylan. *Plant and Cell Physiology*

Luo, M.-C., You, F.M., Li, P., et al. (2015) Synteny analysis in Rosids with a walnut physical map reveals slow genome evolution in long-lived woody perennials. *BMC Genomics*, **16**, 707.

Lyons, E., Pedersen, B., Kane, J. and Freeling, M. (2008) The Value of Nonmodel Genomes and an Example Using SynMap Within CoGe to Dissect the Hexaploidy that Predates the Rosids. *Tropical Plant Biol.*, **1**, 181–190.

Magallón, S., Gómez-Acevedo, S., Sánchez-Reyes, L.L. and Hernández-Hernández, T. (2015) A metacalibrated time-tree documents the early rise of flowering plant phylogenetic diversity. *New Phytologist*, **207**, 437–453.

Manabe, Y., Nafisi, M., Verhertbruggen, Y., et al. (2011) Loss-of-Function Mutation of REDUCED WALL ACETYLATION2 in Arabidopsis Leads to Reduced Cell Wall Acetylation and Increased Resistance to Botrytis cinerea. *Plant Physiology*, **155**, 1068–1078.

Marakli, S. and Gozukirmizi, N. (2018) Analyses of abiotic stress and brassinosteroid-related some genes in barley roots grown under salinity stress and HBR treatments: Expression profiles and phylogeny. *Plant Biosystems - An International Journal Dealing with all Aspects of Plant Biology*, **152**, 324–332.

Marrano, A., Martínez-García, P.J., Bianco, L., et al. A new genomic tool for walnut (Juglans regia L.): development and validation of the high-density Axiom™ J. regia 700K SNP genotyping array. *Plant Biotechnology Journal*, **0**.

Martínez-García, P.J., Famula, R.A., Leslie, C., McGranahan, G.H., Famula, T.R. and Neale, D.B. (2017) Predicting breeding values and genetic components using generalized linear mixed models for categorical and continuous traits in walnut (Juglans regia). *Tree Genetics & Genomes*, **13**, 109.

Masachis, S., Segorbe, D., Turrà, D., et al. (2016) A fungal pathogen secretes plant alkalinizing peptides to increase infection. *Nature Microbiology*, **1**, 16043.

Ming, R., Hou, S., Feng, Y., et al. (2008) The draft genome of the transgenic tropical fruit tree papaya (*Carica papaya* Linnaeus). *Nature*, **452**, 991–996.

Miuishi, T (1946) "In Praise of the Walnut" *Suna no Toride*. Translated from Japanese by T. Lento. *Usui Shobo*.

Moral, J., Muñoz-Díez, C., González, N., Trapero, A. and Michailides, T.J. (2010) Characterization and Pathogenicity of Botryosphaeriaceae Species Collected from Olive and Other Hosts in Spain and California. *Phytopathology*, **100**, 1340–1351.

Oliver, M. (1992) "The Black Walnut Tree". *New and Selected Poems (Volume one). Beacon Press*.

Pina-Martins, F., Baptista, J., Pappas, G. and Paulo, O.S. (2019) New insights into adaptation and population structure of cork oak using genotyping by sequencing. *Global Change Biology*, **25**, 337–350.

Plomion, C., Aury, J.-M., Amselem, J., et al. (2018) Oak genome reveals facets of long lifespan. *Nature Plants*, **4**, 440.

Pope, K.S., Dose, V., Silva, D.D., Brown, P.H., Leslie, C.A. and DeJong, T.M. (2013) Detecting nonlinear response of spring phenology to climate change by Bayesian analysis. *Global Change Biology*, **19**, 1518–1525.

Potter, D., Gao, F., Baggett, S., McKenna, J.R. and McGranahan, G.H. (2002) Defining the sources of Paradox: DNA sequence markers for North American walnut (Juglans L.) species and hybrids. *Scientia Horticulturae*, **94**, 157–170.

Richter, J., Ploderer, M., Mongelard, G., Gutierrez, L. and Hauser, M.-T. (2017) Role of CrRLK1L Cell Wall Sensors HERCULES1 and 2, THESEUS1, and FERONIA in Growth Adaptation Triggered by Heavy Metals and Trace Elements. *Front Plant Sci*, **8**.

Richter, J., Watson, J.M., Stasnik, P., Borowska, M., Neuhold, J., Berger, M., Stolt-Bergner, P., Schoft, V. and Hauser, M.-T. (2018) Multiplex mutagenesis of four

clustered CrRLK1L with CRISPR/Cas9 exposes their growth regulatory roles in response to metal ions. *Scientific Reports*, **8**, 12182.

Simão, F.A., Waterhouse, R.M., Ioannidis, P., Kriventseva, E.V. and Zdobnov, E.M. (2015) BUSCO: assessing genome assembly and annotation completeness with single-copy orthologs. *Bioinformatics*, **31**, 3210–3212.

Singh, D., Bhaganagare, G., Bandopadhyay, R., Prabhu, K.V., Gupta, P.K. and Mukhopadhyay, K. (2012) Targeted spatio-temporal expression based characterization of state of infection and time-point of maximum defense in wheat NILs during leaf rust infection. *Mol Biol Rep*, **39**, 9373–9382.

Singh, R., Ong-Abdullah, M., Low, E.-T.L., et al. (2013) Oil palm genome sequence reveals divergence of interfertile species in Old and New worlds. *Nature*, **500**, 335–339.

Smit, AFA, Hubley, R & Green, P. *RepeatMasker Open-4.0*. 2013-2015 <http://www.repeatmasker.org>.

Stanke, M., Diekhans, M., Baertsch, R. and Haussler, D. (2008) Using native and syntenically mapped cDNA alignments to improve de novo gene finding. *Bioinformatics*, **24**, 637–644.

Stevens, K.A., Woeste, K., Chakraborty, S., et al. (2018) Genomic Variation Among and Within Six Juglans Species. *G3: Genes, Genomes, Genetics*, **8**, 2153–2165.

Sui, S., Luo, J., Liu, D., Ma, J., Men, W., Fan, L., Bai, Y. and Li, M. (2015) Effects of Hormone Treatments on Cut Flower Opening and Senescence in Wintersweet (Chimonanthus praecox). *HortScience*, **50**, 1365–1369.

Tuskan, G.A., DiFazio, S., Jansson, S., et al. (2006) The Genome of Black Cottonwood, Populus trichocarpa (Torr. & Gray). *Science*, **313**, 1596–1604.

Tuskan, G.A., Groover, A.T., Schmutz, J., et al. (2018) Hardwood Tree Genomics: Unlocking Woody Plant Biology. *Front. Plant Sci.*, **9**.

Vijay, N., Poelstra, J.W., Künstner, A. and Wolf, J.B.W. (2013) Challenges and strategies in transcriptome assembly and differential gene expression quantification. A

comprehensive in silico assessment of RNA-seq experiments. *Molecular Ecology*, **22**, 620–634.

Vu, D.C., Lei, Z., Sumner, L.W., Coggeshall, M.V. and Lin, C.-H. (2019) Identification and quantification of phytosterols in black walnut kernels. *Journal of Food Composition and Analysis*, **75**, 61–69.

Vu, D.C., Vo, P.H., Coggeshall, M.V. and Lin, C.-H. (2018) Identification and Characterization of Phenolic Compounds in Black Walnut Kernels. *J. Agric. Food Chem.*, **66**, 4503–4511.

Wagner, T.A. and Kohorn, B.D. (2001) Wall-Associated Kinases Are Expressed throughout Plant Development and Are Required for Cell Expansion. *The Plant Cell*, **13**, 303–318.

Wang, X., Xu, Y., Zhang, S., et al. (2017) Genomic analyses of primitive, wild and cultivated citrus provide insights into asexual reproduction. *Nature Genetics*, **49**, 765–772.

Weckerle, C., Huber, F.K., Yongping, Y. and Weibang, S. (2005) Walnuts among the Shuhi in Shuiluo, Eastern Himalayas. *Economic Botany*, **59**, 287–290.

Xia, Y., Yin, S., Zhang, K., Shi, X., Lian, C., Zhang, H., Hu, Z. and Shen, Z. (2018) OsWAK11, a rice wall-associated kinase, regulates Cu detoxification by alteration the immobilization of Cu in cell walls. *Environmental and Experimental Botany*, **150**, 99–105.

Xu, H., Yu, X., Qu, S. and Sui, D. (2013) Juglone, isolated from Juglans mandshurica Maxim, induces apoptosis via down-regulation of AR expression in human prostate cancer LNCaP cells. *Bioorganic & Medicinal Chemistry Letters*, **23**, 3631–3634.

Yang, Z. (2007) PAML 4: Phylogenetic Analysis by Maximum Likelihood. *Mol Biol Evol*, **24**, 1586–1591.

Yao, Y., Zhang, Y.-W., Sun, L.-G., et al. (2012) Juglanthraquinone C, a novel natural compound derived from Juglans mandshurica Maxim, induces S phase arrest and apoptosis in HepG2 cells. *Apoptosis*, **17**, 832–841.